Article

Modeling and Optimization for Konjac Vacuum Drying Based on Response Surface Methodology (RSM) and Artificial Neural Network (ANN)

Zhiheng Zeng, Ming Chen, Xiaoming Wang, Weibin Wu *, Zefeng Zheng, Zhibiao Hu and Baoqi Ma

College of Engineering, South China Agricultural University, Guangzhou 510642, China;
zengzhiheng@stu.scau.edu.cn (Z.Z.); chenming123@stu.scau.edu.cn (M.C.);
ebianwxm1234@stu.scau.edu.cn (X.W.); scauzzf@stu.scau.edu.cn (Z.Z.); huzhibiao1998@stu.scau.edu.cn (Z.H.);
mabaoqi@stu.scau.edu.cn (B.M.)
* Correspondence: wuweibin@scau.edu.cn; Tel.: +86-20-8528-2269

check for updates

Abstract: To reveal quality change rules and establish the predicting model of konjac vacuum drying, a response surface methodology was adopted to optimize and analyze the vacuum drying process, while an artificial neural network (ANN) was applied to model the drying process and compare with the response surface methodology (RSM) model. The different material thickness (MT) of konjac samples (2, 4 and 6mm) were dehydrated at temperatures (DT) of 50, 60 and 70 °C with vacuum degrees (DV) of 0.04, 0.05 and 0.06 MPa, followed by Box–Behnken design. Dehydrated samples were analyzed for drying time (*t*), konjac glucomannan content (KGM) and whiteness index (WI). The results showed that the DT and MT should be, respectively, under 60 °C and 4 mm for quality and efficiency purposes. Optimal conditions were found to be: DT of 60.34 °C; DV of 0.06 MPa and MT of 2 mm, and the corresponding responses *t*, KGM and WI were 5 h, 61.96% and 82, respectively. Moreover, a 3-10-3 ANN model was established to compare with three second order polynomial models established by the RSM, the result showed that the RSM models were superior in predicting capacity ($R^2 > 0.928$; MSE < 1.46; MAE < 1.04; RMSE < 1.21) than the ANN model. The main results may provide some theoretical and technical basis for the konjac vacuum drying and the designing of related equipment.

Keywords: drying; konjac; vacuum; glucomannan; optimization

1. Introduction

Konjac is one of the most important high glucomannan containing perennial herbs grown in the north of the Indochina peninsula and Yunnan China and which is widely used in medicine, health care and the dyeing industry [1,2]. The newly harvest konjac is perishable, owing to its high moisture content (80–85%) and considerable amounts of the herb are wasted due to the lack of efficient preservation techniques that are unique to konjac [3]. An effective method seems to be drying to obtain a stable konjac product for further use.

Drying plays an important role in extending the shelf life of fleshy agricultural products, and it is a difficult food processing operation mainly because of the undesirable changes in quality of dried products. To maintain the quality of the dried product, various drying methods were proposed to remove the free water to halt or retard the growth of spoilage microorganisms as well as the occurrence of chemical reactions [4–7]. Vacuum drying technology has been widely used in vegetable and fruit drying owing to its high efficiency, heating uniformity and high quality of the dried product [8]. In the last few decades, numerous investigators have examined the vacuum drying characteristics

in vegetables and fruits with a high moisture content, such as lemon slices [9], eggplant [10] and cauliflower [11]. Among the above drying experiments, the dried products show great performance in the color retention and nutritive qualities, which might due to the fact that the oxidation is prevented because the samples have no contact with air during the drying process so that the sensory and nutritive qualities of foodstuffs are effectively maintained [10]. According to the analysis above, the vacuum drying technology is suitable for the postharvest treatment of the fresh konjac, as the fresh konjac slices are easily oxidized.

Recently, further uses of konjac are receiving more and more attention by industries due to its high content of konjac glucomannan. The use of the konjac glucomannan has been reported by several researchers. Iglesias-Otero et al. [12] revealed the influence of a konjac glucomannan aqueous dispersion as ingredient, at different alkalinity levels, on the thermal stability of low-quality squid surimi. As the key operation of the fresh konjac postharvest treatment process, researchers have also paid close attention to the drying technology for konjac. For instance, an experimental study on hot air drying for konjac showed that the drying rate is significantly improved, while the quality is seriously damaged [13]. Kumar et al. [14] developed a kinetic model under different temperatures to describe the konjac moisture content changes during the hot air drying process. Wei et al. [15] also developed a mathematical model for the konjac dying process in a heat pump drying system. A characteristic of the study was that the konjac color was protected by soaking the sample in the color fixative (L-cysteine 0.25 g/L, citric acid 10 g/L, ascorbic acid 0.2 g/L) for 3 min before drying, resulting in the dried product having a stable color. Though researchers have done a lot of work on the drying process of the konjac, few quality change investigations and optimization of drying process parameters for the konjac vacuum drying process have been reported [16].

The response surface methodology (RSM) is one of the most effective tools which is widely used in optimization studies. The methodology extracts quantitative data from an appropriate experimental design to determine and simultaneously solve multivariate problems. The mathematical equations developed by the RSM can describe the effect of test variables on responses, determine interrelationships among test variables and represent the combined effect of all test variables in any response [17]. Accordingly, researchers can have a better understanding of a process or a system. Though the efficiency of the RSM in revealing interrelationships among test variables has been verified in food processes optimization [18–20], the forecasting behavior of the RSM should also be further tested. Artificial neural network is the most widely implemented methodology in forecasting [21]. In some cases, where there is no basis for linear or polynomial process modeling, modeling through an artificial neural network can be a quick and convenient solution. ANN is a data-driven technique, inspired by biological neural systems, able to compute the relationship between input and output variables. In most previous studies, ANN models have been proven to show a better predicting capacity than other models, such as Lewis, Page, and RSM models [22–24]. Comparisons of prediction performance of the ANN models and RSM models were reported in some studies related to chemical industries [25,26], however, there are few studies on comparing the ANN models and RSM models in the food drying process. Based on the background, further modeling for RSM and comparison between ANN models and RSM models are necessary.

To fully understand the drying process and the quality change rule of the dried product for konjac vacuum drying, the RSM was adopted to optimize the main parameters of vacuum drying of konjac. An experiment followed by Box–Behnken design was conducted to investigate the effects of the three process parameters, including drying temperature (DT), material thickness (MT) and vacuum pressures (DV), on the drying time (*t*), konjac glucomannan content (KGM) and whiteness index (WI). Artificial neural network models were established to compare the established RSM models. The main objectives of this study are as follows: (a) To obtain the optimized drying process parameters for konjac vacuum drying; (b) To analyze the influence of interactions between three independents on responses; (c) To develop the predicting models for konjac vacuum drying. This study hopes to lay some theoretical and technical basis for guiding the practical production of the konjac vacuum drying.

2. Materials and Methods

2.1. Sample Preparation

The newly harvested konjac (white konjac annual) was purchased from a local farmer (Yi bin Sichuan province China) and stored in a refrigerator at approximately 4 °C prior to the experiment [23]. The raw konjac samples with similar size and regular shape were selected for the experiment. The konjac samples were trimmed manually into cubes with 2, 4 and 6 mm for the thickness, 5 and 5 mm for the length and width, respectively. The weight of 50 ± 0.1 g for the three thicknesses of the sample were used for the experiment. The original weight of the samples were recorded in advance and then the sized samples were used for testing in the vacuum drying apparatus.

2.2. Equipment and Procedure Description

The experiments were performed in a vacuum drier (DZF-2AS, Beijing kewei yongxing instrument Co., Ltd., Beijing, China), which includes an automatic weighing system (accuracy to 0.001 g), an electrically vacuum system which could provide a negative pressure range from 0.01 MPa to 0.09 MPa, the plate electric heater was inserted into the dry chamber equably in order to offer a stable temperature (maximum to 100 °C) to dry the sample, a power control was used to monitor the energy consumption. The dryer was preheated for almost 1 h before the experiment, which could help to reduce the error caused by thermal inertia. Besides, the activated carbon was placed in the bottom of the container to keep it dry during the experimental period. During the drying experiment, the mesh and samples were weighed at 20 min intervals by a digital electronic balance (Shanghai Jingtian). Each of the experiments was completed three times under the same conditions, and the average values were used for the analysis.

2.3. The Key Indexes of the Konjac Vacuum Drying

2.3.1. Drying Time

The drying time (*t*) of each experiment was measured when the deviations of sample mass in the two successive experiments were less than 0.1 g [27].

2.3.2. Konjac Glucomannan

In the present work, the content of konjac glucomannan (KGM) was assessed by the existing National Standard Spectrophotometry method [28]. In detail, glucomannan is decomposed into two reducing sugars including D-mannose and D-glucose, after hydrolysis, while 3,5-Dinitrosalicylic acid and the reducing sugar co boiling in alkaline solution can produce brown amino compounds. It can be said that the content of the reducing sugar is directly proportional to the color of the reaction solution in a certain range, so the content of reducing sugar in the reaction solution can be measured by spectrophotometry [29]. To ascertain the content of the reducing sugar, a standard curve for glucose should be established to compare with the color of the reaction solution. The standard curve for glucose (Figure 1) and the non-linear equations (Equation (1)) were established in advance in order to calculate the *KGM* content followed by Equation (2).

$$Y = 0.49X^2 + 1.042X + 0.017 \tag{1}$$

where, *Y* is the glucose of the dried product, mg; *X* is absorbance.

$$KGM = 5\varepsilon(5S - H)/m(1 - w) \tag{2}$$

where, *KGM* is the konjac glucomannan content (d.b.%); ε is the ratio of mannose molecular weight to glucose ε = 0.9; *S* is the glucose weight of glucomannan hydrolysate identified by standard curve, mg; *H* is the glucose weight of glucomannan extracting solution identified by standard curve, mg; *m* is the

sample weight, g; w is the moisture content, %; Two replicates for each of the experiment were done and the errors were limited to 5%.
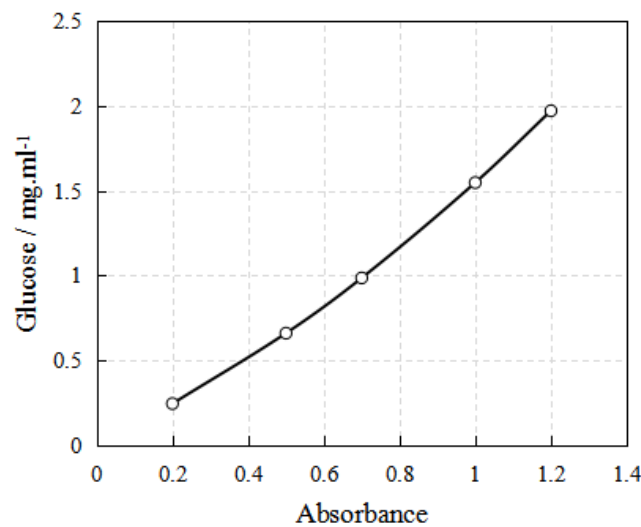

Figure 1. The standard curve of glucose.

2.3.3. Whiteness Index

In the present work, the whiteness index (WI) was applied to describe the color change of the dried konjac samples [30]. The WI of the dried product was measured using HunterLab UltraScan PRO (Eutin international trading Co., Ltd., Shanghai, China), the index of L^*, a^* and b^*, respectively, are darkness degree (black to white: 0~100), redness and greenness degree and (−60~60), and yellowness and blueness degree (−60~60). The WI can be calculated by the following Hunter equation [31]. During the test, the standard white color was used for calibration and the measurements were performed for all dried samples. Besides, each of the experiments was replicated three times for statistical purposes.

$$WI = 100 - \sqrt{(100 - L^*)^2 + a^* + b^*} \qquad (3)$$

2.4. Experimental Design

2.4.1. Response Surface Methodology

In this work, three konjac thicknesses (MT), drying temperatures (DT) and vacuum degrees (DV) were considered to be the independent variables for konjac vacuum drying, while the drying time (t), konjac glucomannan content (KGM) and whiteness index (WI) were regarded as the responses. An experimental design followed by the Box–Benhnken design was performed to analyze the effects of the interaction of independent variables (DT, MT and DV) on the responses (t, KGM and WI) and to optimize the drying process. The experimental design representing the natural and coded values of independent variables is shown in Table 1, and a total 17 experimental runs are shown in Table 2, where there are 5 central point runs in the design. The Design Expert 8.0.6 software was adopted to analyze the interactions of the independent variables on the response, while Matlab R2016a software was applied to establish the ANN model of the konjac vacuum drying. Moreover, a second-order polynomial model (Equation (4)) was used to describe the relationship between the response and the independent variables [11].

$$Y = \beta_0 + \sum_{i=1}^{2} \beta i X i + \sum_{i=1}^{2} \beta i j X_i^2 + \sum_{i=1}^{2} \beta_{ij} X_i X_j \qquad (4)$$

where Y is the response variable, X_i and X_j are the independent variables affecting the response, β_0, β_0 and β_{ij} are the regression coefficients for intercept quadratic liner and interaction terms.

Table 1. Experimental design for vacuum drying of konjac.

Variables	Code Levels		
	−1	0	1
	Natural Levels		
DT (Drying temperatures,°C)	50	60	70
MT (Konjac Thicknesses, mm)	2	4	6
DV (Vacuum Degrees, MPa)	0.04	0.05	0.06

Table 2. Experimental values of response variables for Box–Behnken design.

Run	Std	Experimental Design			Results		
		DT (°C)	DV (MPa)	MT (mm)	*t* (*h*)	KGM (%)	WI
1	10	60(0.5)	0.06(1)	2(0)	5.42(0.06)	62.5(0.99)	81.4(0.97)
2	16	60(0.5)	0.05(0.5)	4(0.5)	6.62(0.34)	52.8(0.43)	75.9(0.70)
3	12	60(0.5)	0.06(1)	6(1)	7.32(0.50)	49.5(0.24)	66.2(0.24)
4	3	50(0)	0.06(1)	4(0.5)	6.75(0.37)	46.8(0.09)	65.8(0.22)
5	4	70(1)	0.06(1)	4(0.5)	5.15(0.00)	52.1(0.39)	73.8(0.60)
6	17	60(0.5)	0.05(0.5)	4(0.5)	6.68(0.35)	52.9(0.44)	76.2(0.72)
7	11	60(0.5)	0.04(0)	6(0.5)	6.95(0.41)	51.06(0.33)	68.7(0.36)
8	6	70(1)	0.05(0.5)	2(0)	5.99(0.19)	51.2(0.34)	70.6(0.45)
9	15	60(0.5)	0.05(0.5)	4(0.5)	7.08(0.44)	53.2(0.45)	76.2(0.72)
10	8	70(1)	0.05(0.5)	6(1)	6.35(0.28)	48.2(0.17)	63.6(0.11)
11	2	70(1)	0.04(0)	4(0.5)	6.54(0.32)	45.32(0.00)	61.3(0.00)
12	13	60(0.5)	0.05(0.5)	4(0.5)	6.65(0.34)	50.8(0.32)	73.5(0.59)
13	7	50(0)	0.05(0.5)	6(1)	9.5(1.00)	48.74(0.20)	65.4(0.20)
14	5	50(0)	0.05(0.5)	2(0)	7.12(0.45)	62.7(1.00)	82.1(1.00)
15	1	50(0)	0.04(0)	4(0.5)	7.67(0.58)	51.51(0.36)	71.8(0.50)
16	9	60(0.5)	0.04(0)	2(0)	6.05(0.21)	54.2(0.51)	78.2(0.81)
17	14	60(0.5)	0.05(0.5)	4(0.5)	6.52(0.31)	54.2(0.51)	76.4(0.73)

Note: The values in bracket are the normalized values. KGM: konjac glucomannan content; WI: whiteness index.

2.4.2. Artificial Neural Network Modeling

In the present work, a feed-forward back propagation ANN model was established to fit the experimental data, the proposed model consists of three kinds of layers: (1) input layer with three neurons related to the independent variables (DT, DV and MT). (2) the number of hidden layers was ascertained to be 10, as described by Li et al., 2016 [32]. The Tansig function is a good tradeoff for neural networks, where speed is important and the exact shape of the transfer function is not [33], accordingly, the Tansig function was adopted to be the transfer function between the hidden layer and the output layer, while the Levenberg–Marquardt algorithm was adopted to be the training function of the network. (3) output layer with neurons associated with the responses (*t*, WI and KGM). As for the training parameters, the number of epochs was ascertained to be 1000 while the momentum coefficient was ascertained to be 0.4. Accordingly, the topological structure of the proposed model can be ascertained to be 3-10-3 (as shown in Figure 2).
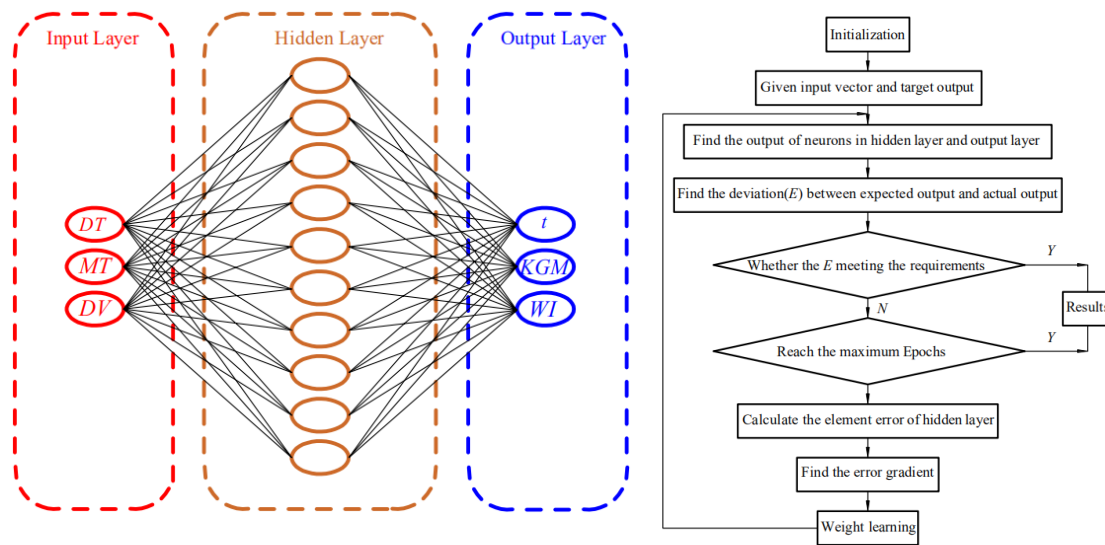
Figure 2. The established BP (Back Propagation) neuron network.

2.5. Statistical Analysis

The experimental data should be normalized before modeling by the ANN model, and the experimental value were processed by the formula: $x_i = (x − x_{min})/(x_{max} − x_{min})$, where, x_i is the normalized value, x is experimental value, x_{max} is the maximal value and x_{min} is the minimum value. The experimental value and the normalized value were tabulated in the Table 2. The performance of the prediction models (RSM models and ANN models) were statistically evaluated by the determination coefficient (R^2), mean absolute error (MAE), mean square error (MSE) and root mean square (RMSE), which can be, respectively, calculated followed by the Equations (5)–(8) [34,35]:

$$R^2 = \frac{\sum_{i=1}^{n} \left(Ypred, i − \overline{Y_{exp}} \right)^2}{\sum_{i=1}^{n} \left(Y_{exp,i} − \overline{Y_{exp}} \right)^2} \tag{5}$$

$$MAE = \frac{1}{n} \sum_{i=1}^{n} \left| Y_{pred,i} − Y_{exp,i} \right| \tag{6}$$

$$MSE = \frac{\sum_{i=1}^{n} \left(Ypred, i − Y\exp, i \right)^2}{n} \tag{7}$$

$$RMSE = \sqrt{MSE} \tag{8}$$

where, $Y_{pred,i}$ is the value predicted by the models, $Y_{exp,i}$ is the experimental value, Y_{exp} is the mean of the experimental values and *n* is the number of the data points.

3. Results

In the present work, the RSM was adopted to investigate the influence of the independent variables (DT, MT and DV) on the dependent variables (*t*, KGM and WI). ANOVA was employed to analyze the significant terms that effect on *t*, KGM and WI, and multiple linear regression analysis of the experimental data yielded second order polynomial model (Equation (4)) for predicting the optimal *t*, KGM, and WI. The *p*-value, Lack of fit, coefficient of variation (C.V.%), coefficient of determination (R^2), Adj R^2, Pred R^2, Adep Precision, PRESS and residuals obtained by the ANOVA were adopted to determine the significance of the terms or the models. A regression equation coefficient of the proposed models with statistical significance of the main responses was calculated for each response and their significance values ($p \leq 0.05$) were judged, as tabulated in Table 3. The interactions of any

two independent variables that effect t, KGM and WI were visualized with the response 3D surface plots for the fitted model as the function of two independent variables. The main results of the effect of the drying parameters on responses are as follows:

Table 3. ANOVA evaluation of linear, quadratic and interaction terms for response and coefficient of prediction models.

Source	Drying Time			Konjac Glucomannan Content			Whiteness Index		
	Sum of Squares	Coefficient	*p*-Value	Sum of Squares	Coefficient	*p*-Value	Sum of Squares	Coefficient	*p*-Value
Model	13.68	3.832	0.0023 *	316.99	52.29	0.0022 *	591.03	5.1375	0.0004 *
DT	6.14	−0.28217	0.0003 *	20.90	0.96962	0.037 *	31.20	3.38	0.0203 *
DV	0.83	498.125	0.0448 *	9.70	−129.125	0.1233	6.48	−287.5	0.2157
MT	3.84	0.83075	0.0012 *	136.95	−9.69875	0.0003 *	292.82	−7.0125	<0.0001 *
DT•DV	0.055	−1.175	0.5482	33.01	28.725	0.0178 *	85.56	46.25	0.0017 *
DT•MT	1.02	−0.02525	0.0301 *	30.03	0.137	0.0144 *	23.52	0.12125	0.0358 *
DV•MT	0.25	12.5	0.2214	24.30	−123.25	0.0276 *	8.12	−71.25	0.1714
DT^2	0.37	2.9525×10^{-3}	0.1479	28.38	−0.025962	0.0201 *	118.83	−0.053125	0.0006 *
DV^2	1.09	−5097.5	0.0262 *	4.14	−9912.5	0.2903	18.79	−21125	0.0536
MT^2	0.17	0.050687	0.3009	32.69	0.69656	0.0148 *	0.08	0.034375	0.8844
Residual		0.97			22.14			24.49	
Lack of Fit		0.83 (NS)			18.35 (NS)			18.91(NS)	
Pure Error		0.15			3.79			5.58	
Std. Dev		0.37			1.78			1.87	
Mean		6.74			52.14			72.17	
R^2		0.9337			0.9347			0.9602	
Adj R^2		0.8485			0.8508			0.9091	
Pred R^2		0.0825			0.1168			0.4943	
Adep Pre		14.499			13.693			14.865	
C.V.%		5.53			3.41			2.59	
PRESS		13.44			299.53			311.28	

Note: "*" characterizes significant terms of the model and "NS" presents not significant.

Based on the ANOVA analysis shown in Table 3, three second order polynomial models (Equations (9)–(11)) were established. The models were further utilized for each response in order to determine the specified optimal drying conditions. Similar methodology has been adopted for optimizing the drying process of *pleurotus eryngii* in a microwave-vacuum dryer [36].

$$t = 3.832 - 0.28217DT + 498.125DV + 0.83075MT - 1.175DT \cdot DV - 0.02525 \\ DT \cdot MT + 12.5DV \cdot MT + 2.9525 \times 10^{-3}DT^2 - 5097.5DV^2 + 0.050687MT^2 \tag{9}$$

$$KGM = 52.29 + 0.96962DT - 129.125DV - 9.69875MT + 28.725DT \cdot DV + \\ 0.137DT \cdot MT - 123.25DV \cdot MT - 0.025962DT^2 - 9912.5DV^2 + 0.69656MT^2 \tag{10}$$

$$WI = 5.1375 + 3.38DT - 287.5DV - 7.0125MT + 46.25DT \cdot DV + 0.12125DT \\ \cdot MT - 71.25DV \cdot MT - 0.053125DT^2 - 21125DV^2 + 0.034375MT^2 \tag{11}$$

3.1. Drying Time

The ANOVA of drying time—shown in Table 3—presents that drying time was significantly affected by the three independent variables and the effects of three factors on drying time in descending order are as follows: drying temperature (DT), material thickness (MT), drying vacuum degree (DV). The terms R^2, Adj R^2, Pred R^2, Adep Precision, C.V.% and PRESS shown in Table 3 are used to check the suitability of the model. It was found that the *p*-value of the model for the drying time is 0.0015, indicating that the model is significant. The value of the determination coefficient (R^2) is 0.9337,

which implies that 93.37% of the variations can be explained by the fitted model. The Adj R^2 of 0.8485 is close to the R^2 of 0.9337. The lack of fit for the model is not significant and a relatively low value of *C.V.* (5.63%) also indicates a good reliability of the experiment's data. In conclusion, the fitted model demonstrates good suitability and can be adopted to describe the variation of the drying time.

It can be seen that an interaction term (DT•MT) and a quadratic term (DV^2) significantly affected the drying time. The combined effect of DT and MT affected the drying time was analyzed with the help of the response surface shown in Figure 3a. It can be obviously observed that drying time reduces with the increase in DT, while the drying time reduces with the reduction in the MT when the DT is under 65 °C. However, as shown in Figure 3b, when the DT is above 65 °C, interestingly the drying time reaches the minimum value (5.12 h), where the MT is 3 mm instead of the thinnest MT (2 mm), which might be caused by the material surface hardening shrinkage phenomenon, as reported by Fengying et al. in *Litchi chinensis Sonn* vacuum and selective far-infrared radiation superheat drying process [37], and similar findings were also reported by Xingyi et al. for *shiitake mushroom* [38], and Li Biansheng et al. for candied prunes [39].

(**a**) (**b**)
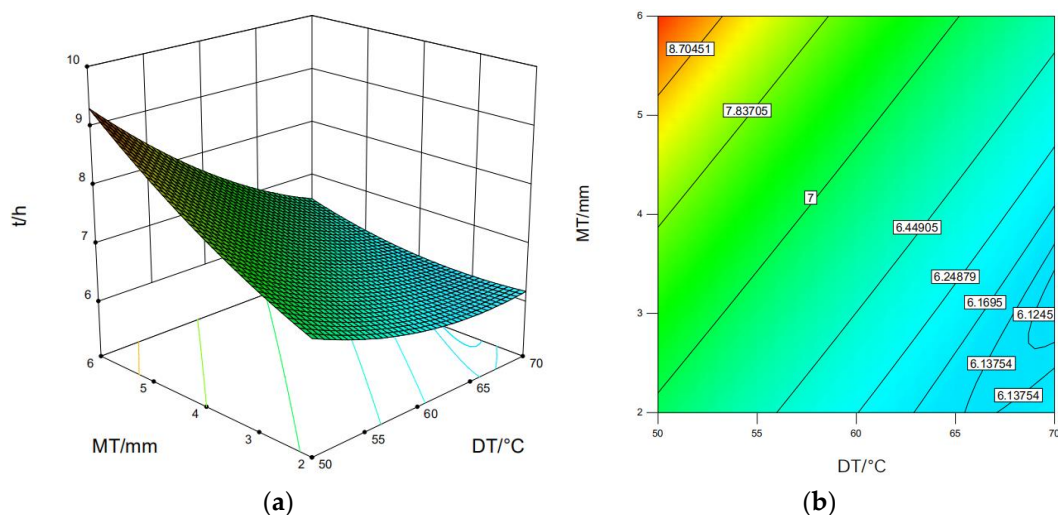
Figure 3. Response surface (**a**) and contour (**b**) for drying time with respect to interaction term DT•MT at a constant vacuum degree of 0.06 MPa.

3.2. Konjac Glucomannan Content

It can be obviously seen from the Table 3 that KGM was significantly affected by the DT, MT, combined effect of MT and DT, MT and DV, DT and DV, DT^2 and MT^2 terms. The values of evaluation indexes including R^2, Adj R^2, Pred R^2, Adep Precision, C.V.% and PRESS are 0.9347, 0.8508, 0.1168, 13.693, 3.41% and 299.53, respectively. The indexes indicate that the model is significant and can be used for further analysis.

Figure 4a depicts the effects of the interaction term DT•DV on the KGM content, the maximum value of KGM content (53.86%) is found at 60 °C and 0.058 MPa for a constant material thickness of 2 mm, as shown in Figure 4b. Figure 5a depicts the effects of the interaction term DT•MT on the KGM content, as can be seen from the figure, the KGM content reaches a lower value when the MT is above 4 mm, in addition to the DT being above 60 °C than that of under 4 mm and 60 °C, respectively, which might have been caused by the negative influence on glue strength when the drying temperature is high, as reported by Iglesias-Otero et al. [12]. The results indicate that the appropriate MT and DT should be under 4 mm and 60 °C in the drying process, and the maximum KGM content is observed when the MT is 2 mm and DT is 50 °C, indicating that a low drying temperature and thin MT might be beneficial to retain the quality of fresh konjac samples, similar results for black turmeric [40], mango cubes [41] and tomato [42] have been reported in the last few years. Figure 6a depicts the effects of the interaction term DV•MT on KGM content, similar to Figure 5a, the KGM value is lower when

the MT is above 4 mm than that of under 4 mm. The optimal KGM content is observed at 0.06 MPa, 2mm with a temperature of 60 °C, as shown in Figure 6b. It can be concluded that a higher vacuum degree and thinner material thickness could promote a drying rate that is conductive to glue strength of the konjac glucomannan content [12].

(**a**)　　　　　　　　　　　　　　　　　　(**b**)
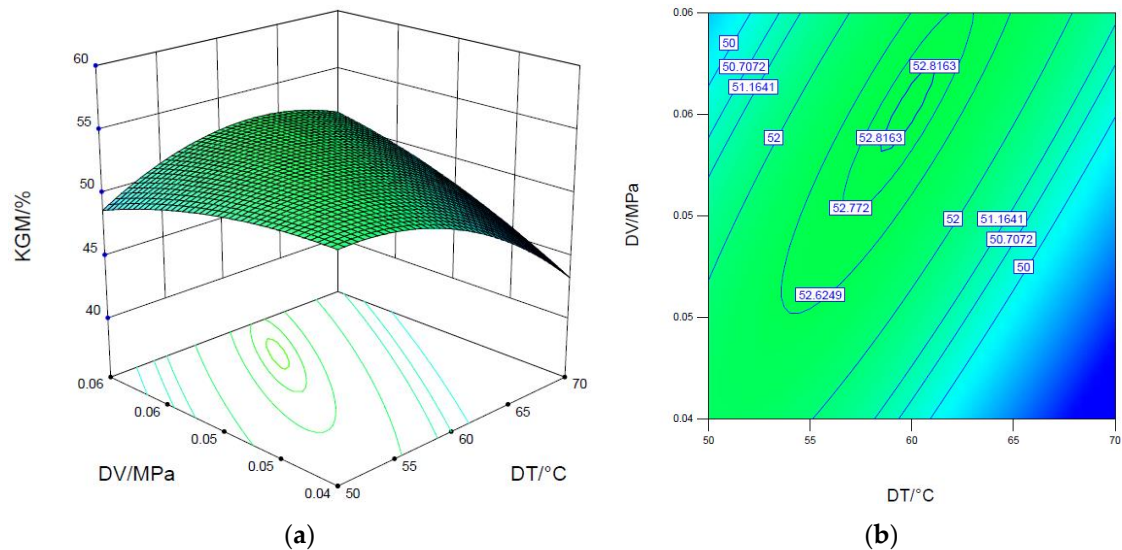
Figure 4. Response surface and (**a**) contour (**b**) for KGM content with respect to interaction term DT•DV at a constant initial material thickness of 2 mm.

(**a**)　　　　　　　　　　　　　　　　　　(**b**)
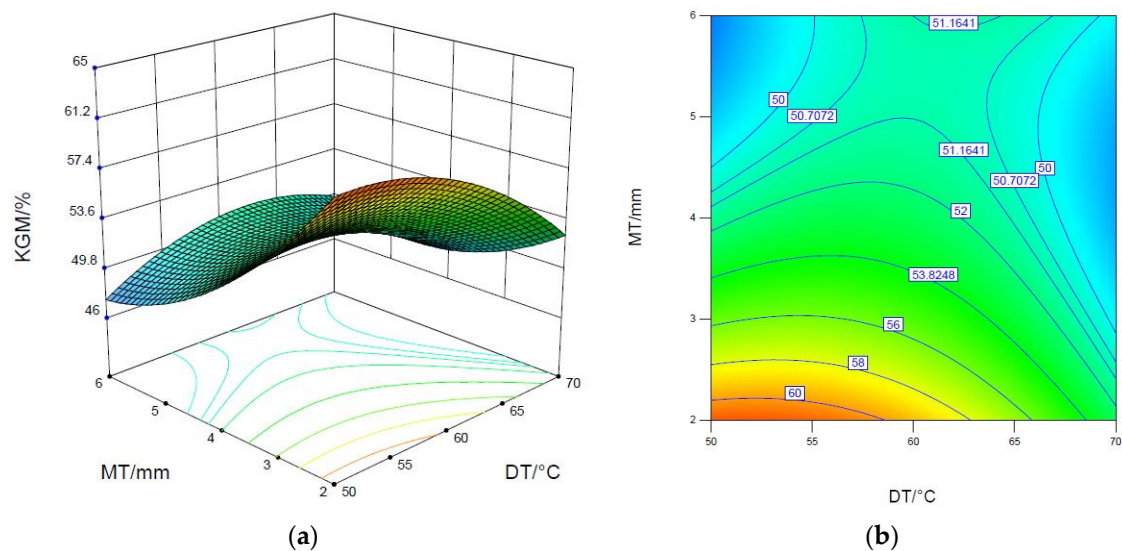
Figure 5. Response surface and (**a**) contour (**b**) for KGM content with respect to interaction term DT•MT at a constant DV of 0.05 MPa.
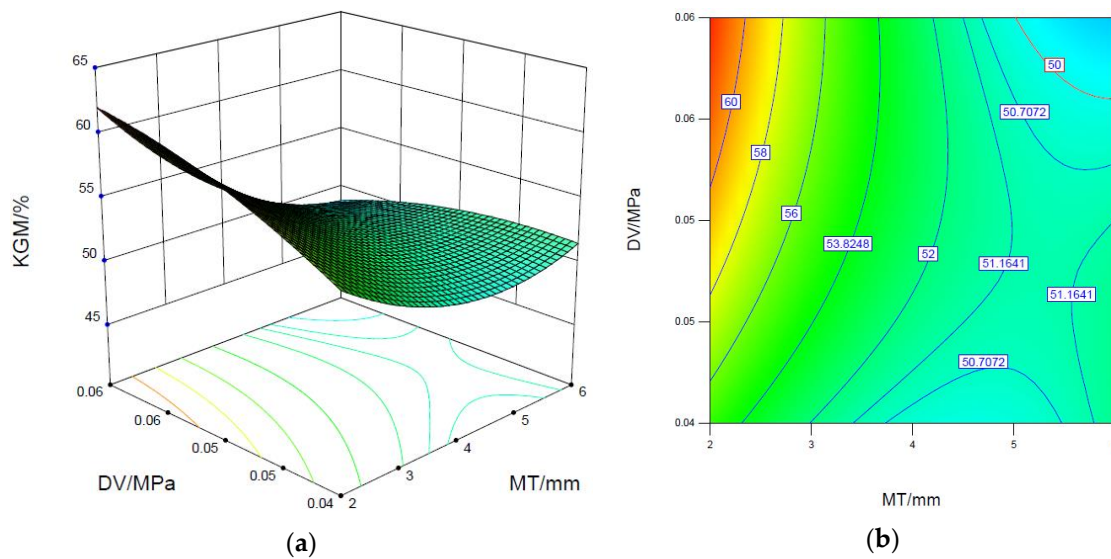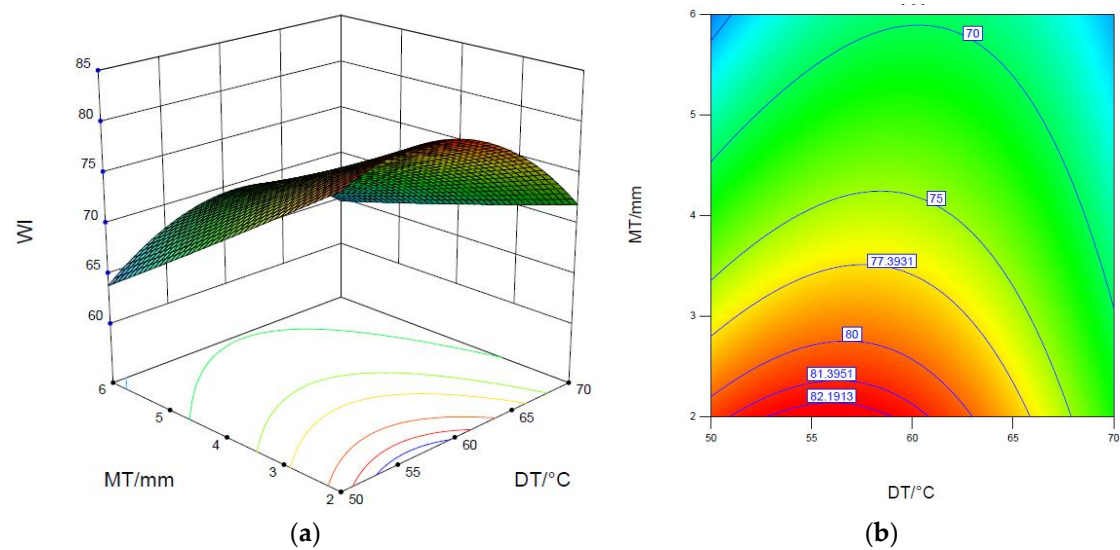
Figure 6. Response surface and (**a**) contour (**b**) for KGM content with respect to interaction term DV•MT at a constant DT of 60 °C.

3.3. Whiteness Index

ANOVA analysis clearly depicts that the WI is significantly affected by the terms of DT, MT, DT•DV, DV•MT and DT^2, the *p*-value (0.0004) of the model shows that the model is significant. Additionally, the significance of the model is also judged by the evaluation indexes mentioned above, and all the behaviors indicate that the model shows good suitability.

Figure 7a depicts the combined effect of MT and DT on WI, obviously it can be seen that the WI increases with the decrease in the MT, it can be deduced that a thinner MT and a proper a DT are favorable for increasing the whiteness index of the sample. The drying time will be extended if the sample is too thick, which might cause the increase in contact time between the samples and the external oxygen, thus intensifying the occurrence of oxidative browning and decreasing the WI. Similar findings have been reported by Song X et al. for infrared drying of Chinese yam [43]. Moreover, the WI increases with the increase in DT when the DT is under 60 °C while WI decreases with the increase in DT when DT is above 60 °C, which might be due to the fact that a higher temperature might make the konjac sample carbonized and further decrease the whiteness index of the sample. As can be seen from the Figure 7b, the optimal value of WI is found to be 82.8 at DT of 57.3 °C and DV of 0.06 MPa, and MT of 2mm, it can be concluded that the drying temperature should be in a reasonable range from 52 to 63 °C. Figure 8 depicts the 3D response surface (a) and the corresponding contour (b) for WI with respect to interaction term DT•DV at a constant MT of 2 mm, as can be seen from the figure, the WI gets the optimal value (75.8) when the DT is 57.3 °C, DV is 0.05 MPa and MT is 2 mm.

Figure 7. Response surface (**a**) and contour (**b**) for WI with respect to interaction term of DT•MT at a constant drying vacuum of 0.06 MPa.
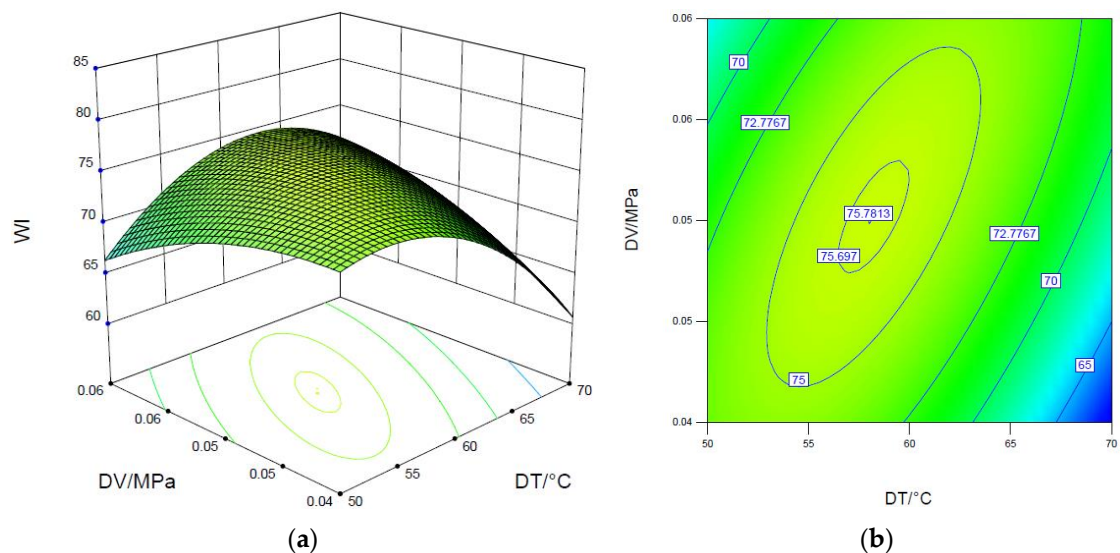
Figure 8. Response surface (**a**) and contour (**b**) for W with respect to interaction term of DT•DV at a constant MT of 2 mm.

3.4. Optimization of Process Parameters

Optimal drying conditions for konjac vacuum drying were determined on the basis of the following criteria: maximum KGM, minimum *t* and maximum WI. The optimization function in the software was applied to optimize the drying parameters in the range of 50–70 °C for drying temperature, 0.04–0.06 MPa for vacuum degree and 2–6 mm for material thickness. As tabulated in Table 4, five solutions are found for the optimum covering criteria with a desirability value above 0.980—by using the desirability function method. A similar methodology has been applied for olive leaves drying optimization [44]. The optimized variables were close to each other such as drying temperature, drying vacuum and material thickness varied between 58.73–61.58 °C, 0.06–0.06 MPa and 2.00–2.00 mm, respectively. Although all the five solutions are similar, the best optimized conditions obtained for the given criteria are 60.34 °C, 0.06 MPa and 2.00 mm on the basis of maximum desirability (0.984). For the optimized combination of drying parameters, the predicted *t*, KGM and WI are 5 h, 61.96% and 82, respectively.

Table 4. Optimization solutions for the konjac vacuum drying.

Solution Number	Parameters			Responses			Desirability
	DT	MT	DV	t	KGM	WI	
1	60.34	2.00	0.06	5	61.96	82	0.984
2	59.92	2.00	0.06	5	62.03	82	0.983
3	60.99	2.00	0.06	5	61.82	82	0.981
4	60.37	2.02	0.06	5	61.85	82	0.980
5	58.73	2.00	0.06	5	62.17	82	0.980

3.5. ANN Modeling for Konjac Vacuum Drying

Based on the established 3-10-3 artificial neural network in Section 2.4.1, the 17 sets of experimental data shown in Table 2 were used for the training, and the training results are depicted in the following Figure 9. As can be seen from the figure, the ANN model shows the best training performance when the training epochs are two, where the MSE of the model is 0.00545, the R values for the train, validation and test data, respectively, are 0.960, 0.959 and 0.952, indicating that the established ANN model has sufficient reliability and can be used for predicting the drying performance of the konjac vacuum drying. Moreover, to achieve the repeatability of the model, the weights of the established ANN model are listed in the Table 5.

Figure 9. The training results of the 3-2-10-3 artificial neural network (ANN) model.

Table 5. The weights of the established model.

Weight	Matrix
$iw\{1,1\}$	$\begin{bmatrix} -1.5485 & -1.1896 & 1.2995 & -0.1283 & 0.88355 & -1.8239 & -1.0092 & 1.4292 & 2.3875 & 1.5284 \\ -2.2486 & -1.6935 & -2.3644 & -0.16251 & -2.8041 & 1.7806 & -2.2935 & -2.0127 & -0.1276 & 1.6143 \\ -1.0057 & -1.705 & -1.1219 & -2.883 & 0.22473 & 1.4881 & 0.49466 & -1.8236 & -1.1918 & -2.2426 \end{bmatrix}^T$
$iw\{2,1\}$	$\begin{bmatrix} 0.11719 & -0.20031 & -0.92857 & 0.24623 & 0.25743 & 0.50884 & 1.1206 & -0.16612 & 0.87807 & 0.12095 \\ -0.24653 & 0.28233 & 0.44907 & 1.1557 & -0.2302 & 0.46417 & 0.42098 & -0.55108 & -0.6603 & 0.801 \\ 0.19157 & 0.4472 & 0.93092 & 0.97381 & -1.0095 & 0.6018 & -0.017862 & 0.097757 & -0.30043 & -0.15305 \end{bmatrix}$
$b\{1\}$	$\begin{bmatrix} 3.1099 & 2.5969 & -1.7251 & 1.1526 & 0.52729 & -0.82056 & -1.0568 & 1.5445 & 2.8732 & 2.869 \end{bmatrix}^T$
$b\{2\}$	$\begin{bmatrix} -0.415334 & 0.70893 & 0.32821 \end{bmatrix}^T$

3.6. Comparison of the Established RSM Models and the ANN Model

Based on the ANOVA analysis shown in Table 3, three second order polynomial models (Equations (9)–(11)) were established. The experimental data were fitted by the established RSM models and the ANN model, and the comparison of values predicted by RSM models, ANN models and experimental values are presented in Figure 10, and the performance of the models were evaluated by the specific evaluation criterion (R^2, MAE, MSE and RMSE), and the results are tabulated in Table 6.
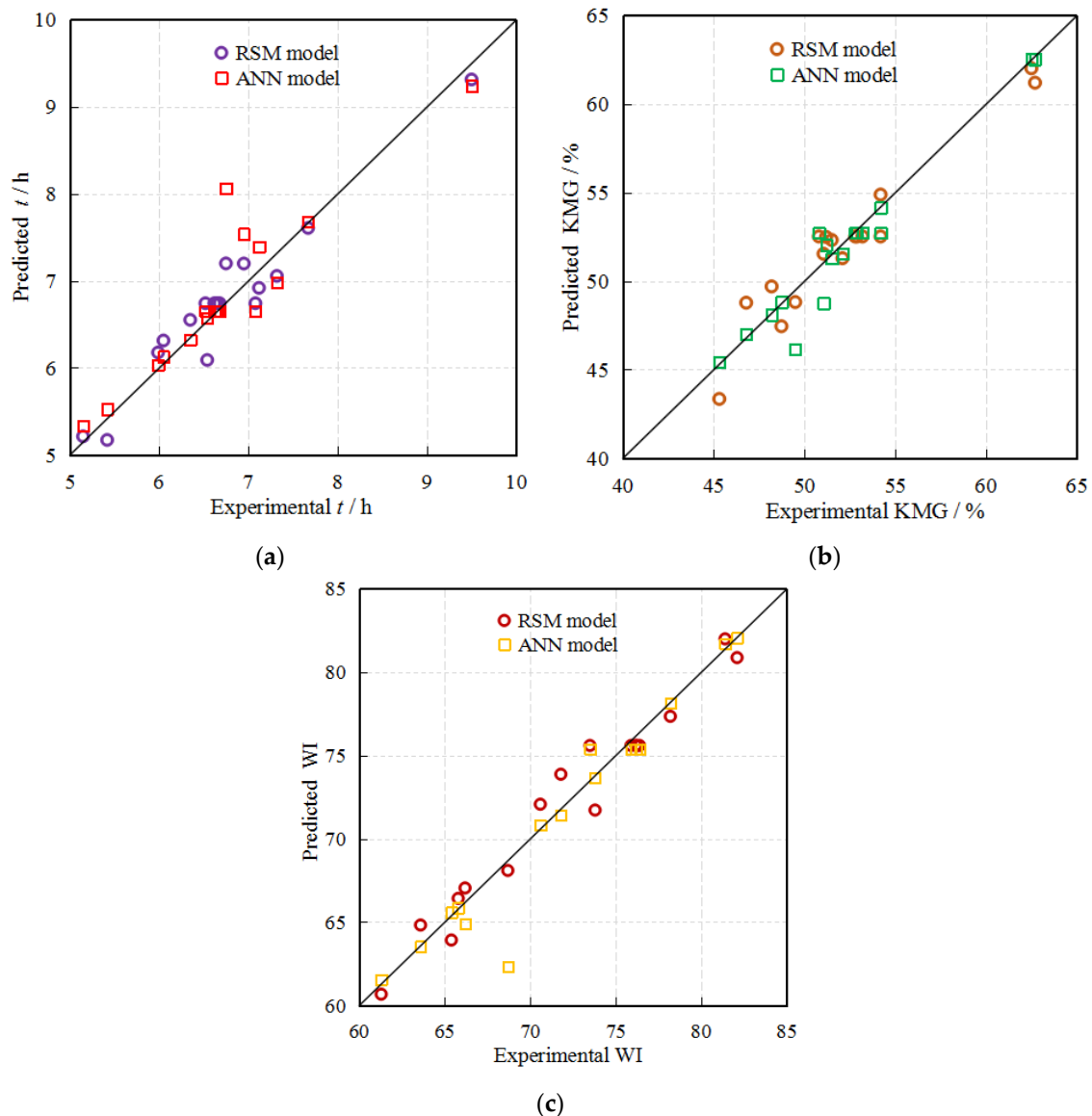
Figure 10. The comparison of experimental values and predicting results for the *t* (**a**), KMG (**b**) and WI (**c**). RSM: response surface methodology.

Table 6. Statistical parameters for comparing RSM and ANN models.

Parameters	RSM Models			ANN Model		
	t **(h)**	**KGM (%)**	**WI**	*t* **(h)**	**KGM (%)**	**WI**
Determination coefficient (R^2)	0.9312	0.9286	0.9591	0.9796	0.9982	0.9896
Mean-square error (MSE)	0.0595	1.4399	1.4648	0.2116	2.5676	6.2089
Mean absolute error (MAE)	0.2092	1.0262	1.0427	0.1823	0.6773	1.2922
Root-mean-square error (RMSE)	0.2439	1.1999	1.2103	0.4600	1.6024	2.4918

The artificial neural network model often shows a better prediction ability in some reported studies [45–48], however, RSM models are demonstrated to have a better predicting ability than ANN models in the present work. Obviously, it can be seen from the Figure 10 that the experimental plots are closer to the RSM curves than to the ANN one. The error of RSM model ranges between −0.453~0.449 h, −1.98~1.97% and −2.1~2.15 for the *t*, KGM and WI, respectively, while the error of the ANN model ranges −0.37~1.82 h, −1.35~5.96% and −2.66~7.41 for the *t*, KGM and WI, respectively, which indicates the errors of the values predicted by the RSM model are within a smaller range than by the ANN model. In other words, the established RSM models showed a better predicting ability than the established 3-10-3 ANN model.

The statistical results of the parameters for comparing RSM and ANN models are tabulated in Table 6, as can be seen from the table, the values of R^2 for the three RSM models vary from 0.929 to 0.959, while the values of R^2 for the ANN model are all greater than 0.980. However, the values of MAE, MSE and RMSE for RSM models are smaller than the values of corresponding responses predicted by the ANN model. The same behavior was reported by Thyagarajan, et al. [49], who introduced a comparable performance of ANN and RSM models in phytase production modeling. Above all, it can be concluded that the predicting ability of the RSM model is better than the ANN model in the present work and the established RSM models may provide some practical guidance for the konjac vacuum drying process.

4. Conclusions

In the present work, RSM was adopted to analyze the drying process and optimize the drying conditions for konjac vacuum drying. Artificial neural network was applied to compare he established RSM models. The main conclusions, depending on the results of the present work, are summarized as follows:

(1) Three second order polynomial models (KGM, *t*, WI) were established in this study, though the models show good predicting performance, the results at the significance level showed that the WI performs a better performance than the KGM and *t*.

(2) The results of the interaction analysis indicated that the drying temperature and the material thickness of the konjac should be, respectively, under 60 °C and 4 mm for quality and efficiency purposes.

(3) The optimal drying conditions obtained based on the given criteria are 60.34 °C, 0.06 MPa and 2.00 mm. For the optimized combination of drying parameters, the *t*, KGM and WI are 5 h, 61.96% and 82, respectively. In order to facilitate the practical production, the optimal drying parameters were adjusted as 60.00 °C, 0.06 MPa and 2.00 mm.

(4) Though both models provided good quality predictions, the results confirmed that the established RSM models in this work are superior in predicting capacity compared ($R^2 > 0.928$; MSE < 1.46; MAE < 1.04; RMSE < 1.21) with the ANN model. Such a result may suggest that the performance may be a problem-specific issue and might provide some theoretical and technical basis for guiding the konjac vacuum drying and the designing of related equipment.

Conflicts of Interest: The authors declare that we have no known competing financial interests or personal relationships that could have appeared to influence the work reported in this paper.

References

1. Li, W.; Zheng, H.; Bukuru, J.; De Kimpe, N. Natural medicines used in the traditional Chinese medical system for therapy of diabetes mellitus. *J. Ethnopharmacol.* **2004**, *92*, 1–21. [CrossRef]
2. Diao, T.; Wu, X.; Wu, J.P. The research progress of konjac. *Anhui Agric. Sci. Bull.* **2006**, *6*, 137–139.
3. Niu, Z.; Wang, L.; Sun. Research and utilization of konjac (amorphophallus) resources in china. *J. Southwest Agric. Univ. (Nat. Sci.)* **2005**, *5*, 69–73.
4. Orikasa, T.; Koide, S.; Okamoto, S.; Imaizumi, T.; Muramatsu, Y.; Takeda, J.I.; Shiina, T.; Tagawa, A. Impacts of hot air and vacuum drying on the quality attributes of kiwifruit slices. *J. Food Eng.* **2014**, *125*, 51–58. [CrossRef]
5. Jing-Kun, Y.; Wu, L.X.; Qiao, Z.R.; Cai, W.D.; Ma, H. Effect of different drying methods on the product quality and bioactive polysaccharides of bitter gourd (*momordica charantia* L.) slices. *Food Chem.* **2019**, *271*, 588–596. [CrossRef]
6. Turkmen, F.; Karasu, S.; Karadag, A. Effects of Different Drying Methods and Temperature on the Drying Behavior and Quality Attributes of Cherry Laurel Fruit. *Processes* **2020**, *8*, 761. [CrossRef]
7. Khaled, A.Y.; Kabutey, A.; Selvi, K.Ç.; Mizera, Č.; Hrabe, P.; Herák, D. Application of Computational Intelligence in Describing the Drying Kinetics of Persimmon Fruit (*Diospyros kaki*) During Vacuum and Hot Air Drying Process. *Processes* **2020**, *8*, 544. [CrossRef]
8. Zhong, X.; Kan, L.; Xin, H.; Qin, B.; Dou, G. Thermal effects and active group differentiation of low-rank coal during low-temperature oxidation under vacuum drying after water immersion. *Fuel* **2019**, *236*, 1204–1212. [CrossRef]
9. Wang, J.; Law, C.L.; Nema, P.K.; Zhao, J.H.; Liu, Z.L.; Deng, L.Z. Pulsed vacuum drying enhances drying kinetics and quality of lemon slices. *J. Food Eng.* **2018**, *224*, 129–138. [CrossRef]
10. Wu, L.; Orikasa, T.; Ogawa, Y.; Tagawa, A. Vacuum drying characteristics of eggplants. *J. Food Eng.* **2007**, *83*, 422–429. [CrossRef]
11. Gupta, M.; Sehgal, V.K.; Arora, S. Optimization of drying process parameters for cauliflower drying. *J. Food Sci. Technol.* **2011**, *50*, 62–69. [CrossRef]
12. Manuel, A.I.; Javier, B.; Clara, A.T. Use of Konjac glucomannan as additive to reinforce the gels from low-quality squid surimi. *J. Food Eng.* **2010**, *101*, 281–288. [CrossRef]
13. Qiu, L. An experimental study on air drying properties for thin layer-sliced Konjak. *Acta Univ. Agric. Boreali-Occident.* **1995**, *23*, 78–82.
14. Vishal, K.; Manish, K.; Sanjay, K. Influences of Temperature-Time Blanching on Drying Kinetics and Quality Attributes of Yam Chips. *J. Agric. Eng.* **2012**, *2*, 72–75.
15. Ye, W.; Li, B.G. Drying Characteristics and Mathematical Modeling for Heat Pump Drying of Konjacs. *Sichuan Food Ferment.* **2015**, *51*, 32–36.
16. Zhang, R.; Wang, X.; Li, L.; Cheng, M.; Zhang, L. Optimization of konjac glucomannan/carrageenan/nano-SiO$_2$ coatings for extending the shelf-life of *Agaricus bisporus*. *Int. J. Biol. Macromol.* **2019**, *122*, 857–865. [CrossRef]
17. Swasdisevi, T.; Devahastin, S.; Sa-Adchom, P. Mathematical modeling of combined far-infrared and vacuum drying banana slice. *J. Food Eng.* **2009**, *92*, 100–106. [CrossRef]
18. Burande, R.R.; Kumbhar, B.K.; Ghosh, P.K.; Jayas, D.S. Optimization of fluidized bed drying process of green peas using response surface methodology. *Dry. Technol.* **2008**, *26*, 920–930. [CrossRef]
19. Kumar, G.V.; Agarwal, S.; Asif, M.; Fakhri, A.; Sadeghi, N. Application of response surface methodology to optimize the adsorption performance of a magnetic graphene oxide nanocomposite adsorbent for removal of methadone from the environment. *J. Colloid Interface Sci.* **2017**, *497*, 193–200. [CrossRef]
20. Yuan, Y.; Tan, L.; Xu, Y. Optimization of Combined Drying for Lettuce Using Response Surface Methodology. *J. Food Process. Preserv.* **2016**, *40*, 1027–1037. [CrossRef]
21. Neto, A.H.; Fiorelli, F.A.S. Comparison between detailed model simulation and artificial neural network for forecasting building energy consumption. *Energy Build.* **2008**, *40*, 2169–2176. [CrossRef]

22. Sarimeseli, A.; Coskun, M.A.; Yuceer, M. Modeling microwave drying kinetics of thyme (*thymus vulgaris* L.) leaves using ann methodology and dried product quality. *J. Food Process. Preserv.* **2014**, *38*, 558–564. [CrossRef]

23. Li, B.; Peng, G.-L.; Wu, S.-F.; Luo, C.-W.; Qiu, G.-Y.; Yang, L. Vacuum drying characteristics and modeling of kinetics for konjac. *Food Ferment. Ind.* **2017**, *43*, 115–122. [CrossRef]

24. Sahin, U.; Ozturk, H.K. Comparison between artificial neural network model and mathematical models for drying kinetics of osmotically dehydrated and fresh figs under open sun drying. *J. Food Process Eng.* **2018**, *41*, e12804. [CrossRef]

25. Bas, D.; Boyaci, I.H. Modeling and Optimization II: Comparison of Estimation Capabilities of Response Surface Methodology with Artificial Neural Networks in a Biochemical Reaction. *J. Food Eng.* **2007**, *78*, 846–854. [CrossRef]

26. Desai, K.M.; Survase, S.; Saudagar, P.S.; Lele, S.S.; Singhal, R.S. Comparison of artificial neural network (ANN) and response surface methodology (RSM) in fermentation media optimization: Case study of fermentative production of scleroglucan. *Biochem. Eng. J.* **2008**, *41*, 266–273. [CrossRef]

27. Giri, S.K.; Prasad, S. Drying kinetics and rehydration characteristics of microwave-vacuum and convective hot-air dried mushrooms. *J. Food Eng.* **2007**, *78*, 512–521. [CrossRef]

28. He, Z.-K.; Zhao, G.-H.; Li, M.-T.; Wang, X.-Y.; Li, C.-P. Selenization of konjac glucomannan oligosaccharides by dry heating in the presence of selenite and antioxidant activity of selenized products. *Food Science* **2013**, *34*, 5–9. [CrossRef]

29. Yuan-Ming, S.; Pei-Ying, L.; Sheng-Lin, Z. Spectrophotometry for Glucomannan from *Amorphophallus* spp. *Plant Physiol. Commun.* **1991**, *27*, 219–222.

30. Xiao, H.W.; Yao, X.D.; Lin, H.; Yang, W.X.; Meng, J.S. Effect of SSB (superheated steam blanching) time and drying temperature on hot air impingement drying kinetics and quality attributes of yam slices. *J. Food Process Eng.* **2012**, *35*, 370–390. [CrossRef]

31. Fakhreddin, S.; Mahdi, K. Modeling of moisture loss kinetics and color changes in the surface of lemon slice during the combined infrared-vacuum drying. *Inf. Process. Agric.* **2018**, *5*, 516–523. [CrossRef]

32. Li, B.; Peng, G.L.; Luo, C.W.; Meng, G.D.; Yang, L. Vacuum drying kinetics characteristics of Chinese prickly ash based on Weibull distribution. *Food Ferment. Ind.* **2017**, *43*, 58–64. [CrossRef]

33. Vogl, T.P.; Mangis, J.K.; Rigler, A.K.; Zink, W.T.; Alkon, D.L. Accelerating the convergence of the backpropagation method. *Biol. Cybern.* **1988**, *59*, 257–263. [CrossRef]

34. Chokphoemphun, S. Moisture content prediction of paddy drying in a fluidized-bed drier with a vortex flow generator using an artificial neural network. *Appl. Therm. Eng.* **2018**, *145*, 630–636. [CrossRef]

35. Li, B.; Li, C.; Huang, J. Application of artificial neural network for prediction of key indexes of corn industrial drying by considering the ambient conditions. *Appl. Sci* **2020**, *10*, 5659. [CrossRef]

36. Thyagarajan, R.; Narendrakumar, G.; Kumar, V.R.; Namasivayam, K.R. Comparison of response surface methodology and artificial neural networks for optimization of medium constituents for enhancement of phytase production from hypocrea lixii surt01. *Res. J. Pharm. Technol.* **2016**, *4*, 1–3. [CrossRef]

37. Xu, F.Y.; Li, C.Y.; Chen, Z. Drying Characteristics of Vacuum and Selective Far-Infrared Radiation Superheat for Litchi chinensis Sonn. *J. Huazhong Agric. Univ.* **2009**, *28*, 495–499. [CrossRef]

38. Li, X.; Liu, Y.; Gao, Z.; Xie, Y.; Wang, H. Computer vision online measurement of shiitake mushroom (*lentinus edodes*) surface wrinkling and shrinkage during hot air drying with humidity control. *J. Food Eng.* **2020**, *292*, 110253. [CrossRef]

39. Li, B.; Liu, W.; Li, D.; Yu, Y.; Liu, Y. Characteristics of hot air drying of candied prunes and representation model. *Trans. Chin. Soc. Agric. Eng.* **2009**, *25*, 330–335. [CrossRef]

40. Lakshmi, D.V.N.; Muthukumar, P.; Layek, A.; Nayak, P.K. Drying kinetics and quality analysis of black turmeric (*curcuma caesia*) drying in a mixed mode forced convection solar dryer integrated with thermal energy storage. *Renew. Energy* **2018**, *120*, 23–34. [CrossRef]

41. Sehrawat, R.; Nema, P.K.; Kaur, B.P. Quality evaluation and drying characteristics of mango cubes dried using low-pressure superheated steam, vacuum and hot air drying methods. *LWT* **2018**, *92*, 548–555. [CrossRef]

42. Brooks, M.S.; El-Hana, N.H.A.; Ghaly, A.E. Effects of tomato geometries and air temperature on the drying behavior of plum tomato. *Am. J. Appl. Sci.* **2008**, *5*, 1369–1375. [CrossRef]

43. Song, X.; Hu, H.; Zhang, B. Drying characteristics of chinese yam (*dioscorea opposita thunb*.) by far-infrared radiation and heat pump. *J. Saudi Soc. Agric. Sci.* **2018**, *17*, 290–296. [CrossRef]

44. Chen, J.; Lin, H.; Lin, Y.; Li, H.; Wang, Z. Optimized technology of *pleurotus eryngii* by microwave-vacuum drying based on quality and energy consumption. *Trans. Chin. Soc. Agric. Eng.* **2014**, *30*, 277–284. [CrossRef]

45. Erbay, Z.; Icier, F. Optimization of hot air drying of olive leaves. using response surface methodology. *J. Food Eng.* **2009**, *91*, 533–541. [CrossRef]

46. Rafigh, S.M.; Yazdi, A.V.; Vossoughi, M.; Safekordi, A.A.; Ardjmand, M. Optimization of culture medium and modeling of curdlan production from Paenibacillus polymyxa by RSM and ANN. *Int. J. Biol. Macromol.* **2014**, *70*, 463–473. [CrossRef] [PubMed]

47. Ebrahimpour, A.; Rahman, R.; Ean Ch'ng, D.; Basri, M.; Salleh, A. A modeling study by response surface methodology and artificial neural network on culture parameters optimization for thermostable lipase production from a newly isolated thermophilic *Geobacillus* sp. strain ARM. *BMC Biotechnol.* **2008**, *8*, 96. [CrossRef]

48. Yang, L.B.; Zhan, X.B.; Zhu, L.; Gao, M.J.; Lin, C.C. Optimization of a low-cost hyperosmotic medium and establishing the fermentation kinetics of erythritol production by *Yarrowia lipolytica* from crude glycerol. *Prep. Biochem. Biotechnol.* **2015**, *46*, 376–383. [CrossRef]

49. Mohamed, M.S.; Tan, J.S.; Mohamad, R.; Mokhtar, M.N.; Ariff, A.B. Comparative Analyses of Response Surface Methodology and Artificial Neural Network on Medium Optimization forTetraselmissp. FTC209 Grown under Mixotrophic Condition. *Sci. World J.* **2013**, *36*, 1–14. [CrossRef]